Flow period influence on uranium and trace elements release in water from the waste rock pile of the former La Commanderie uranium mine (France)

A. Martin, Catherine Landesman, A. Lépinay, C. Roux, Julie Champion, P. Chardon, Gilles F Montavon

Flow period influence on Uranium and trace elements release in water from the waste rock pile of the former *La Commanderie* Uranium mine (France)

A. Martin[a], C. Landesman[a]*, A. Lépinay[b], C. Roux[a], J. Champion[a], P. Chardon[c], G. Montavon[a]

[a] SUBATECH, UMR 6457 (IMT-Atlantique, Université de Nantes, CNRS-IN2P3), 4 rue Alfred Kastler, 44307 Nantes, France

[b] Université de Nantes/OSUNA, UMR 3281, 2 rue de la Houssinière, 44322 Nantes Cedex, France

[c] LPC, UMR 6533 (IN2P3/CNRS/Université Clermont Auvergne), 4 avenue Blaise Pascal TSA60026, CS60026, 63178 Aubière Cedex, France

*Corresponding author: Tel: + 33 2 51 85 84 13; Email address: catherine.landesman@subatech.in2p3.fr

Flow period influence on Uranium and trace element release in water from the waste rock pile of the former *La Commanderie* Uranium mine (France)

[redacted]

1. Introduction

After 60 years, uranium mining activities ceased in France during the 1990's, leaving as a legacy over 200 uranium sites involved in uranium production primarily in granitic areas (Chapot *et al.*, 2010). These mining operations have exposed uranium ore and mine tailings to the surface, where the release of radionuclides into the environment has been facilitated by weathering at rates exceeding those typically found in nature (Abdelouas, 2006; Boekhout *et al.*, 2015). Therefore, radionuclides and especially uranium concentrations in water may exceed local background levels close to these former mining sites (Landa and Gray, 1995). Environmental conditions can generate the acid mine drainage (AMD) leaching of uranium that often gets associated with elevated concentrations of highly toxic heavy metals, which act as a major source of both surface and ground water contamination (Abdelouas, 2006).

Given the complexity of uranium release into the environment, each former uranium mining site must be studied as a specific case as regards the local context (radiological, geological and hydrological, plus weather and any specific rehabilitation) (Boekhout *et al.*, 2015; Cuvier *et al.*, 2015; Salbu *et al.*, 2013). For example, at mine sites with heavy rainfall, the water balance is controlled by the weather and the liquid effluent discharge is

typically impossible to control (Pereira *et al.*, 2018). In France, continuous monitoring of the environment and especially water discharge around former uranium mines has been prescribed by regulatory authorities with the potential use of effluent treatment solutions to reduce environmental releases.

The impact of uranium release into the environment is mitigated by the geochemical speciation of uranium, which influences its solubility, mobility and biological availability (Abdelouas, 2006; Duff *et al.*, 2002). In freshwaters, uranium is mainly transported in dissolved form, such as U(VI) species in acidic waters and as ternary calcium-U-carbonate complexes in neutral alkaline waters. Moreover, in the presence of natural organic matter, uranium complexes with fulvic and humic acids (Franke *et al.*, 2000) may be adsorbed onto inorganic particles of various sizes as Fe-oxyhydroxides. However, under the reducing conditions that may exist in a mine tailings depository due to confinement and microbial activity, U(IV) species precipitates as highly-insoluble UO_2 phases (Abdelouas, 2006).

Several techniques have been used to investigate uranium speciation at various levels, including filtration techniques and diffusive gradient in thin films (DGT). Filtration techniques have been employed to estimate the bioavailable fraction of metals based on size exclusion. The 0.45 µm cutoff is the main operative discriminating fraction representing the separation between dissolved plus colloidal species and particles (Menegario *et al.*, 2017). The DGT technique has been applied *in situ* to assess the bioavailable fraction of metals for freshwater organisms (Zhang and Davison, 2015). Briefly, this technique relies on a device that accumulates metal species on a binding agent (Chelex®-100 binding phase) after diffusion through a gel layer and a protective membrane filter (0.45 µm). The protective membrane filter operates a first selection of metal species by size exclusion and the gel layer induces a selection of mobile and labile species defined as DGT-labile fraction. The term labile denotes metal species that can interconvert, within the timescale of their diffusional transport, to a form that can bind. Those metal species include free ions and small organic and inorganic complexes (Menegario *et al.*, 2017; Zhang and Davison, 2015). A comparison between filtered and DGT-labile fractions serves to evaluate the contribution of colloids or inert species (Drozdzak *et al.*, 2016a; Menegario *et al.*, 2017). A number of limitations dictate DGT use under specific environmental conditions with high ion content (Drozdzak *et al.*, 2015; Gimpel *et al.*, 2001; Turner *et al.*,

2012). However, the technique has been previously implemented in a uranium mining environment (Drozdzak *et al.*, 2016a) under alkaline conditions or in an acid mine drainage (AMD)-impacted environment (Casiot *et al.*, 2009).

In this study, a radiological investigation of the area surrounding the former uranium mine at La Commanderie has been carried out in order to identify the environmental footprint and potential anomalies by means of gamma-ray mapping. Based on these results, a field water sampling campaign was performed over nearly 1 year (2016-17), and physicochemical parameters, uranium and trace element concentrations (Sr, Mn, Fe, As) were all measured in four locations. The potential influence of seasonal variability was studied through interpreting results by flow period in accordance with rainfall monitoring. This study has also focused on determining the labile U fraction with the DGT technique in streams and mining waters. The DGT-labile part of U has been compared both with fractionation by filtration at 0.45 µm, 0.1 µm and 0.02 µm of water samples and with local geochemical background and environmental standards.

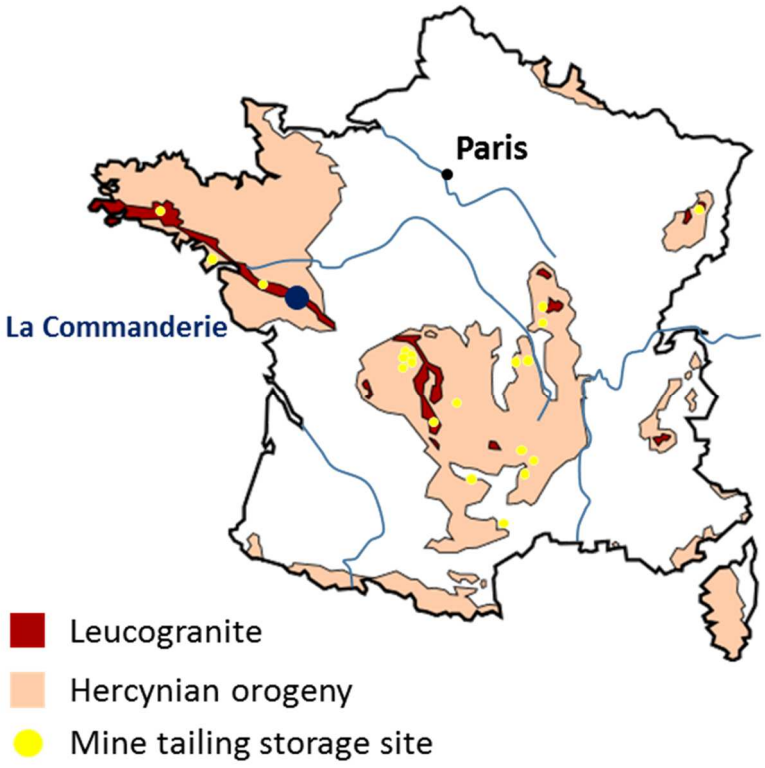

Figure 1: Locations of mine tailing storage sites, including La Commanderie (Hercynian leucogranite area) in France

2. The La Commanderie site

2.1. Location

The former La Commanderie uranium mine is located in western France near the village of "Le Temple" (approx. 450 population), in the vicinity of "Mauléon" right on the border of the "Vendée" and "Deux-Sèvres" Departments (Fig. 1). The main economic activities around La Commanderie consist of farming and industry (Fig. 2). The climate is temperate oceanic, with an average annual temperature of 11°C and average annual rainfall of about 760 mm (*Météo France,* Weather Agency, Risk Prevention Division).

Figure 2: Aerial photographs of the La Commanderie site: a) at the end of the period of mining operations; and b) after the first rehabilitation (AREVA, 2013; Chapot *et al.*, 2010)

2.2. Geological setting and mining activities

The La Commanderie mine deposit is located at the eastern boundary of the Mortagne batholith transected by a regionally defined fault called "Le Temple"; it has been formed in a granitic bedrock, more specifically a plutonic igneous rock consisting essentially (close to 80%) of quartz and feldspar. Uranium in the ore was predominantly present in primary uranium minerals such as pitchblende (Chapot *et al.*, 2010).

The mining site was operated from its discovery in 1955 near the farm of La Commanderie until 1990 as part of France's CEA nuclear program (run by the National Atomic Energy Commission). During the site's operational period, a total of 8.618 million tons (Mt) of ore and mine tailings were extracted for a cumulative U production of 3.644 thousand tons (kt) (Chapot *et al.*, 2010). Roughly 4.96 Mt of tailings were stored adjacent to the waste rock pile on the western side of the site (Figs. 2 and 3). Uranium ore was extracted either by

underground mining operations (1955-1990) or through the open-pit mine (1964-1977). In 1969, the low U content mine tailing was treated by means of a heap leaching process (i.e. static percolation of sulfuric acid) in the northern area of the site (Fig. 3); a settling pond was specifically created to collect the effluent (Fig. 3). The mine was considered “dry”, with a volume of water pumped out between 8 and 30 $m^3.h^{-1}$ to prevent flooding; therefore, few connections with the groundwater system were to be expected.

The site was closed in 1991, but remediation had already started in 1988. The underground mine (< 215 m) and some wells were partially filled with both sand from former gold mines (La Bellière, Saint Pierre Monlimart) and centrifuged sands (0.15 to 0.45 mm) from the Ecarpière site (AREVA, 2013).

The open-pit mine was first filled with tailings from the dismantled heap leaching area and then covered by 10 cm of limestone and 0.7 to 1 m of mine tailings. Over the years, this mine has been gradually filled with water due to precipitation and from the La Commanderie stream (through an artificial water channel). In 2014, solar panels were installed on top of the waste rock pile on the northern and western sides of the basin in order to rehabilitate unused spaces (Fig. 3). The area is now covered by natural vegetation.

At present, the La Commanderie basin extends about 500 m long, 250 m wide and 110 m deep (with 40 m of water). Since 2007, it has been used as water reservoir for irrigation by farmers during the dry season (Fig. 3). The La Commanderie site's current hydrographic network consists of the La Commanderie stream, which wraps around the site from north to south via the eastern side, and a trench skirting along the waste rock pile to the west adjacent to a footpath in order to collect rainwater (Fig. 4). The trench and La Commanderie stream merge at Point B2 (Fig. 4). Downstream, the La Commanderie stream flows into the “Boisdroitière” stream and further down into the “Sèvre Nantaise” River around 4 km from the La Commanderie site.

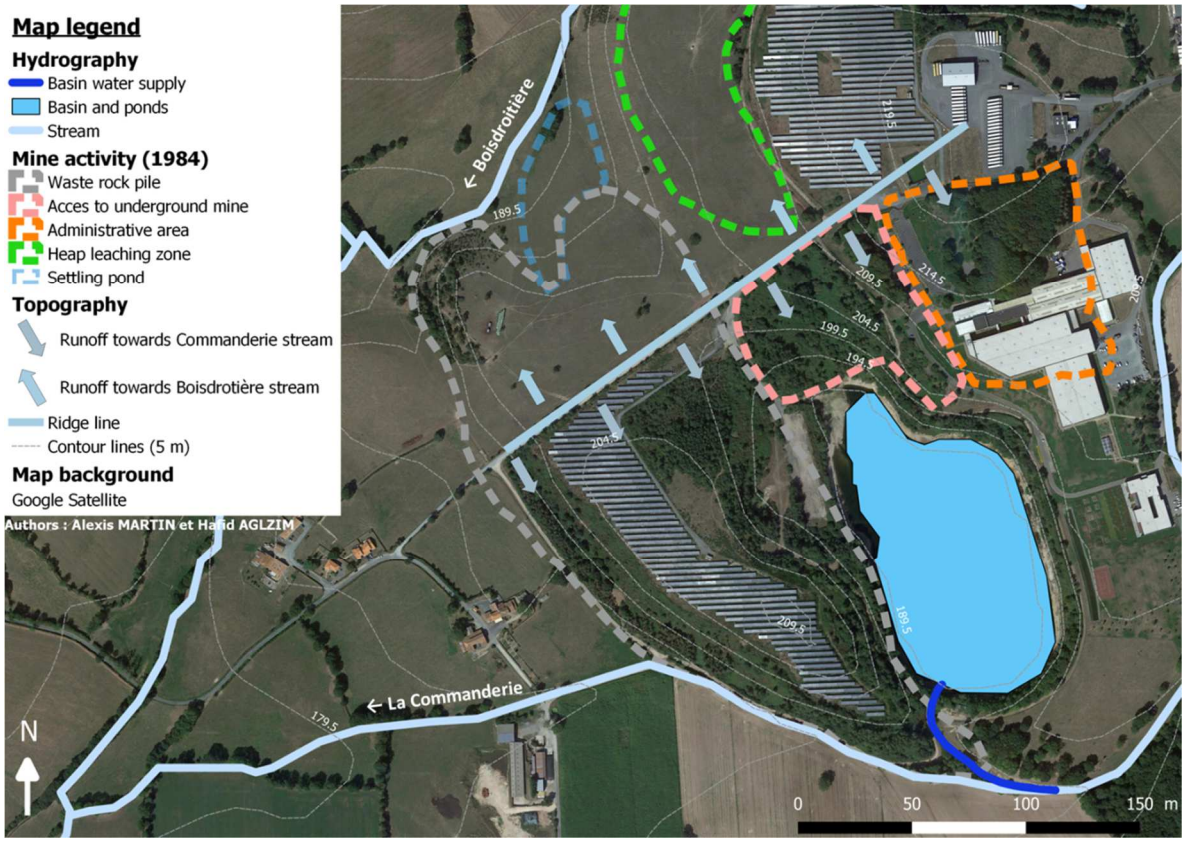

Figure 3: Aerial photography of the La Commanderie site in 2017 with the water-filled former mine and solar panels. The places of former mining activities (1984), the current stream course and water runoff have all been highlighted.

3. Materials and methods

3.1. Radioelement mapping by means of gamma-ray spectrometry

Since the La Commanderie site is a restricted access area, the radiological status was set up in April 2015 and June 2016 all around the site on footpaths accessible to the public. The focus was directed along the periphery of the basin and waste rock pile. Gamma-ray mapping was obtained with SG-2R gamma-ray sensors (Canberra Inc.). The device used coupled the gamma-ray sensor with a Colibri® device (also from Canberra Inc.). Data were acquired automatically every 30 s, and the sensors were placed 1 m from ground level.

3.2. Water sampling and in situ measurements

A preliminary water sampling campaign was performed in January 2016 in order to choose the sampling points on the basis of gamma-ray map results. Four water sampling points C,

B1, B2 and A (Fig. 4) were selected to evaluate the impact of the waste rock pile on the La Commanderie stream. Point C (N 46°55'12.2'' W 000°49'33.2'') was set as a reference representative of the local geochemical background, while Point A (N 46°55'12.2'' W 000°50'12.1'') served to represent the hydrological contamination of La Commanderie stream upstream of the Boisdroitière stream. Water samples were collected monthly from April 2016 to February 2017 (except for November 2016) to assess the impact of seasonal variations on water quality. Spot samples from water seepage (WS) were also collected during overflow observed in March 2018.

Water samples were collected in 2L HDPE bottles after 3 rinses, and subsamples were taken for various analyses. A portion of the sample was sequentially filtered on-site with 0.45, 0.1 and 0.02 µm pore size membrane syringe filters (Sartorius CA 0.45; Sartorius Minisart High Flow PES 0.1 hydrophilic and Whatman Inorganic membrane Anatop™ 25, respectively), in storing a portion of each collected fraction. A preliminary study was performed to evaluate the sorption onto filters. For subsamples dedicated to trace metal and cation analyses, the pH was adjusted in-field to pH 3-4 with ultra-pure HNO_3. All water samples were then stored at -4°C until analysis.

The other parameters, such as temperature, pH, Eh, conductivity and dissolved O_2, were measured *in situ* using a CyberScan PCD 650 multi-parameter instrument and CyberScan pH 110 meter (Eutech Instruments) coupled to dedicated probes. The in-field measurement of alkalinity as HCO_3^- was conducted quickly after sampling by titration using a titration kit (Hach).

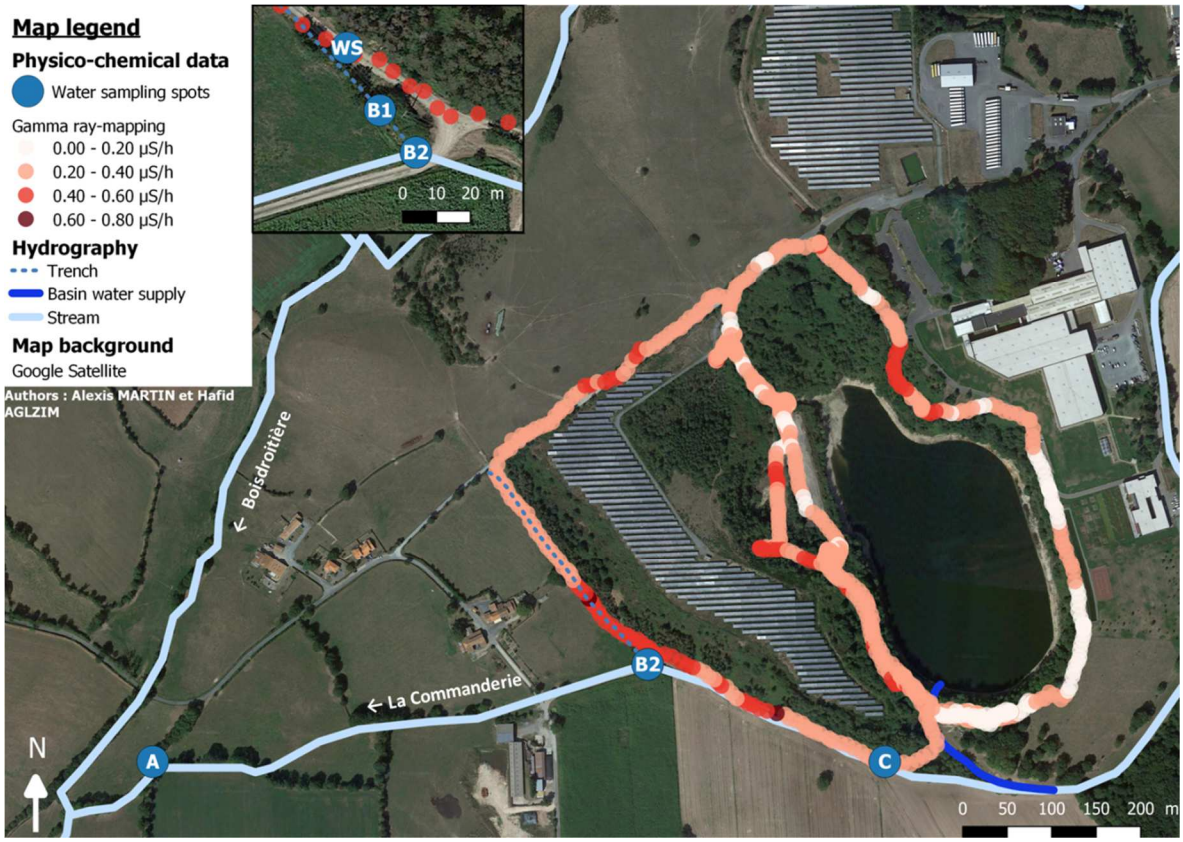

164

165 Figure 4: Map of the present La Commanderie site, with water sampling locations and the
166 gamma-ray map (close-up view on the intersection between trenches and stream).

167 *3.3. Deployment of DGT passive samplers*

168 DGT passive samplers were purchased from DGT Research®; they were of standard
169 configuration (LSNM model) with a protective membrane filter (PES), a polyacrylamide
170 diffusive gel and Chelex®-100 resin gel, offering an exposure area of 3.14 ± 0.06 cm². Before
171 use, these samplers were stored at 4°C in a plastic bag containing a few drops of 0.01M
172 $NaNO_3$. The DGT were deployed in duplicate at each sampling point for approximately 4 h.
173 The apparent flow velocities were sufficient to ensure optimal exposure conditions (Zhang and
174 Davison, 2015).

175 After deployment, the protective membrane filter was rinsed with ultra-pure water. DGT
176 resin gel layers were separated from the device either in-field or in the laboratory on the same
177 day and eluted with 1 mL of 1M HNO_3 for at least 24 h before analysis. DGT field blanks
178 and laboratory blanks were also analyzed to account for deployment and elution steps.

180 The DGT concentration of labile U in water was calculated according to Equation 1:

$$C_{DGT} = m_U \Delta_{gel} / (D_{gel} A t) \quad (1)$$

181 where m_U is the mass of U trapped in the Chelex® resin (µg) corrected for elution
182 efficiency, Δ_{gel} the total thickness of the diffusion layer and protective membrane filter
183 (Δ_{gel} = 0.905 ± 0.0014 mm), D_{gel} the temperature-corrected diffusion coefficient of U
184 through the diffusive gel layer ($cm^2\ s^{-1}$) using the Stokes-Einstein Equation, A the exposure
185 area (sampling window), and t the device deployment time. The elution efficiency of U
186 was experimentally determined to equal 0.84 ± 0.04 under our experimental conditions
187 (data not shown). No consensus was found in the literature on the value of the uranium
188 diffusion coefficient in polyacrylamide diffusive gel due to the various uranium forms
189 found in natural waters and the potential interferences from other ions present at high
190 concentrations (Drozdzak *et al.*, 2015; Hutchins *et al.*, 2012; Turner *et al.*, 2012). We
191 opted for the value derived by Gregusova and Docekal, i.e. $D_{gel} = 4.39 \pm 0.08 \times 10^{-6}$ $cm^2\ s^{-1}$
192 at 25°C and pH = 6.4, who investigated the influence of carbonates on U distribution
193 coefficients in Chelex resin gel discs. Moreover, this value is in good agreement with those
194 reported in several studies (Drozdzak *et al.*, 2015, 2016b; Hutchins *et al.*, 2012).

195 ### *3.4. Analysis of water and DGT*

196 Anion (F^-, Cl^-, SO_4^{2-}, NO_3^-, Br^-, PO_4^{3-}) and cation (Na^+, K^+, Mg^{2+}, Ca^{2+}) concentrations
197 were analyzed by means of ion chromatography (850 Professional IC, Dionex and ICS-
198 1000 IC, Metrohm). Dissolved Organic Carbon (DOC) was measured as Non Purgeable
199 Organic Carbon (NPOC) in acidified samples (filtered at 0.45 µm) with a TOC meter
200 (TOC VCSH, Shimadzu).

201 Trace element concentrations (Mn, Fe, Cu, As, Sr, Pb and U) were analyzed by Inductively
202 Coupled Plasma Mass Spectrometry (ICP XSERIES 2, ThermoFisher Scientific). Matrix
203 effects were minimized by diluting the samples in 2% HNO_3 (2 to 100-fold). Si and Fe
204 were analyzed in collision chamber mode (addition of H/He gas).

205 4. Results and discussion

4.1. Hydrodynamics of the La Commanderie site

The contour lines obtained by a digital field model (see Fig. 3), connecting the parts of a field at equal heights with a 5-m scale, serve to estimate the surface and underground flow directions. Due to the slope, water runoff on the waste rock pile is directed from the NE side into the basin and from the SW side into the trench or the La Commanderie stream (Fig. 3). Runoff onto the former settling pond and heap leaching zone is directed westerly into the Boisdroitière stream. The direct infiltration of rainwater into the waste rock pile must also be considered since stagnant water has been observed at the top of the pile (SI-2). The presence of water in the underground mining galleries is strongly suspected due to former underground mining work that may have crossed soil aquifers and now be saturated with water subsequent to the discontinuation of water pumping.

Field observations highlight that a few meters away, at upper Point B1, an underground drain crossing the footpath from the direction of the waste rock pile is flowing into the trench (SI-2) at a flow rate measured below 80 $L.h^{-1}$. At the same point, seasonal water seepage was observed running over the footpath from the waste rock pile to empty into the trench (SI-2). Moreover, the trench between Points B1 and B2 is covered by visible orange precipitates (SI-2); this phenomenon is not observed in the upper part of the trench not influenced by water seepage.

With the contour lines and overview of the basin (Fig. 3), we observed that the basin altitude is approximately the same (190 m) as the west road following the waste rock pile, although the water level can change with the seasons. Moreover, an investigation of aerial photographs from 1950 (SI-1) suggests that the La Commanderie stream was diverted due to mining activities. The former stream bed reported in SI-1 crossed from the northeast side to the southwest side under both the actual basin and the waste rock pile close to the water seepage location. Therefore, the hypothesis of a hydraulic connection under or inside the waste rock pile between the basin and the water seepage seems reasonable.

In conclusion of the field observations, the water level of the basin and the water seepage flow rate appear to be interconnected and season-dependent. When water seepage overflows the footpath, the basin level reaches its highest values with inflow from rainfall and the water channel. Then, during low-flow periods, water seepage is interrupted as the lowest water level values were observed with evaporation and water use for irrigation.

Rainfall data at Mauléon and flow rate data for the "Sèvre Nantaise" River at the closest recording station (around 20 km upstream) were reported in SI-3 and SI-4 for the purpose of estimating both high and low-flow periods for the years 2016 and 2017 (DREAL, Loire Valley Regional Environmental and Planning Agency). The flow rate estimated from point-specific flow velocity measurements and water levels in the stream at the Point B2 location range from 10 to 100 $m^3.h^{-1}$ depending on the season. With respect to the monitoring period, the first high-flow period corresponds to samples collected before July 2016 (HF1), while the associated low-flow period corresponds to samples collected between July and October 2016 (LF) and a second high-flow period after November 2016 (HF2). The flow rate measured in the "Sèvre Nantaise" River during the HF2 period was significantly less than HF1 (SI-3) due to a severe drought during summer and autumn 2016 (SI-4). The occurrence of water seepage appears to be seasonally correlated, with a flow rate estimated in the field at around 500 $L.h^{-1}$, and could be controlled by managing water filling of the basin during high-flow periods.

4.2. Gamma-ray mapping

The results of gamma-ray mapping are shown in Figure 4, with a color scale extending from 0.1 to 0.8 $\mu S.h^{-1}$. The survey on accessible footpaths distinguishes different radioactivity levels. The geochemical background, below 0.2 $\mu S.h^{-1}$, was measured in the eastern part of the basin, where no excavation works or storage was performed to the best of our knowledge of the mine's operating history. Around the waste rock pile, a radioactivity level between 0.2 and 0.4 $\mu S.h^{-1}$ has been detected, which remains close to the background level. Note that for purposes of public health policy, these values lie below the regulatory limit of 1 mSv/year under a scenario of 400 h/year exposure; hence, no risk to the public was ever considered (AREVA, 2013).

Two hotspots show a radioactivity level 3 times that of the local background: the northern part of the basin, where a former well was used to transport equipment and materials from the surface to the underground mine; and southwest of the waste rock pile where local water seepage was observed during high-flow periods. These observations were decisive in both choosing the water sampling points and identifying water seepage as the potential source of radionuclide leaks into the water. We thus elected to focus our investigation on the La Commanderie stream between Points C and A along with an additional sampling

point B1 (N 46°55'16.1'' W 000°49'46.3''). This approach reflected the direct contribution of water seepage via the trench and Point B2 (N 46°55'15.7'' W 000°49'45.8'') at the mixing point between the trench and the stream.

4.3. Hydrogeochemistry

The water sampling points (C, B1, B2 and A) were selected by virtue of the localized water seepage (WS), which is the most probable source of radionuclides responsible for the local gamma hotspots. The corresponding monitoring was performed during a nearly one-year period between 2016 and 2017 in order to evaluate the seasonal impact. As an initial step, the main parameters (pH, Eh, conductivity, dissolved O_2, DOC and temperature) were measured to characterize: the water from the La Commanderie stream (C, B2, A), WS, and their mix in the trench (B1). The dataset is listed in Table 1, with average values per hydrological period and the associated inner variability expressed as a standard deviation.

Table 1: Average values of water quality parameters and fluoride concentrations (with SD in brackets) from the La Commanderie stream at sampling Points C, B1, B2 and A during both high-flow (HF1, n=3 and HF2, n=4) and low-flow (LF, n=3) periods.

			pH			**Eh (mV_{NHE})**			**σ (µS.cm^{-1})**		
Site/Flow period			HF1	LF	HF2	HF1	LF	HF2	HF1	LF	HF2
C			6.7 (0.2)	6.6 (0.1)	6.3 (0.2)	278 (15)	312 (46)	278 (15)	174 (18)	201 (37)	208 (46)
B1			6.6 (0.2)	6.5 (0.3)	6.1 (0.1)	234 (27)	50 (62)	220 (58)	271 (36)	544 (58)	530 (47)
B2			6.7 (0.1)	6.9 (0.2)	6.4 (0.1)	231 (42)	155 (70)	153 (110)	213 (35)	217 (35)	263 (45)
A			6.6 (0.2)	6.6 (0.2)	6.2 (0.1)	243 (40)	127 (175)	131 (60)	228 (36)	253 (59)	302 (52)
Dissolved O_2 (mg.L^{-1})			**DOC (mg.L^{-1})**			**Temperature (°C)**			**[F$^-$] (mg.L^{-1})**		
HF1	LF	HF2	HF1	LF	HF2	HF1	LF	HF2	HF1	LF	HF2
7 (1.3)	6.3 (1.2)	6.7 (0.7)	4.7 (0.2)	5.8 (0.6)	6.6 (0.7)	10.8 (3.6)	10 (2)	6.8 (1.6)	0.26 (0.01)	0.31 (0.06)	0.23 (0.01)
6.8 (0.6)	0.9 (0.4)	2.6 (1.5)	5.2 (0.1)	10.8 (3.8)	7.2 (4.9)	10.7 (1.3)	13.5 (1.3)	7.7 (2)	1.3 (0.5)	1.3 (0.09)	1.3 (0.2)
7.6 (0.7)	8 (1)	7.7 (0.7)	5 (0.2)	6.2 (0.5)	6.6 (0.5)	10.6 (1.2)	10.3 (2.1)	6.8 (2)	0.6 (0.1)	0.43 (0.05)	0.39 (0.08)
6.3 (2.3)	6.9 (2.7)	3.1 (1.8)	5 (0.3)	7.6 (2.2)	33.5 (15.2)	10.9 (2.4)	10.6 (1.9)	7 (1.9)	0.6 (0.04)	0.4 (0.04)	0.36 (0.07)

pH measurements in the water seepage and underground drain water were conducted in March 2018 (HF period). Results show acidic values of pH (4.20 and 4.25, respectively) in comparison with the stream water (Table 1). The stream water pH is in fact slightly acidic ($6.0 < pH < 7.1$) for surface waters, with the lowest values observed at Point B1 in the trench. The contribution of water seepage during HF periods is likely responsible for a slight decrease in pH. The Eh measurements demonstrate a change at Point B1 during the

LF period, with values close to reductive conditions in the trench. The conductivity (σ) was relatively low although higher σ values were also recorded at Point B1 (544 and 533 $\mu S.cm^{-1}$). Dissolved oxygen values in the stream correspond to 50-80% of the expected value (equilibrium with the atmosphere) for surface waters, and anoxic conditions were detected during the LF period at B1. Since the La Commanderie stream originates around 1 km upstream of the La Commanderie site (Fig. 3), these readings may be insufficient to ensure complete equilibrium. The dissolved organic carbon (DOC) levels lie below 10 $mg.L^{-1}$, as would be expected for surface waters (Rodier et al., 2009), and an increase has been noticed at Point A during HF2 with an average value of 33.5 $mg.L^{-1}$. The water composition characterization was complemented by an ion analysis report as average concentrations in Figure 4 for F^- and Figure 5 for both anions (Cl^-, HCO_3^- + CO_3^{2-}, SO_4^{2-} +NO_3^-) and cations (Na^++K^+, Mg^{2+}, Ca^{2+}).

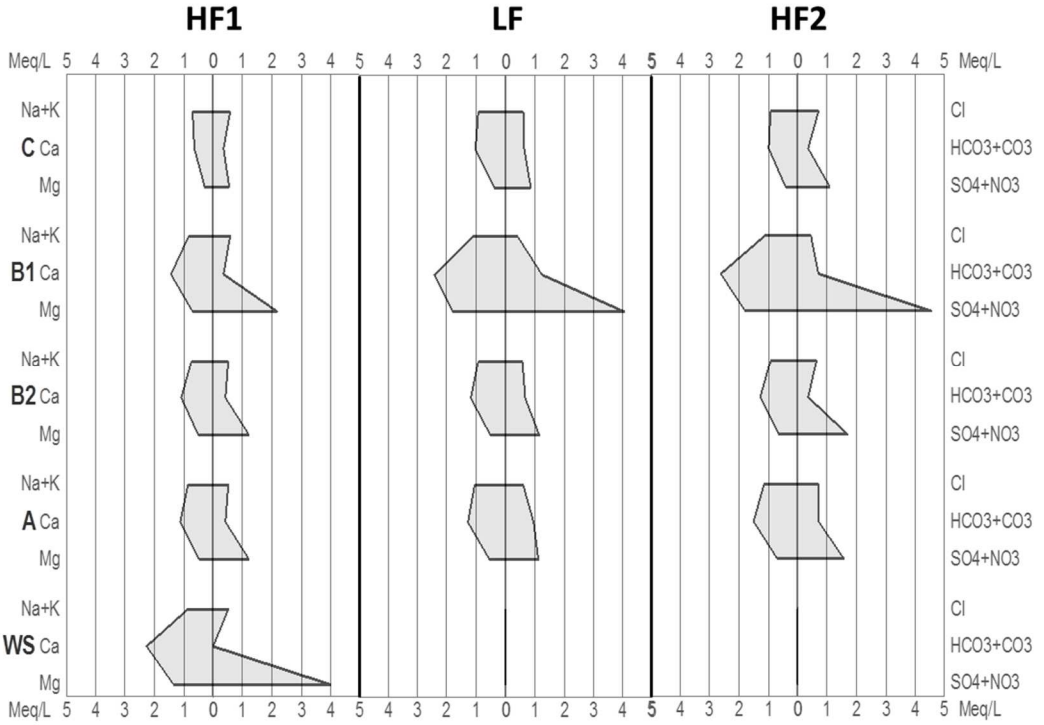

Figure 5: Stiff diagrams with average cation (Na^++K^+, $Ca2^+$, Mg^{2+}) and anion (Cl^-, HCO_3^-+CO_3^{2-}, SO_4^{2-}+NO_3^-) concentrations in $meq.L^{-1}$ for C, B1, B2, A and WS water samples during both high and low-flow periods

Water ion balances are equilibrated for all sampling points with 10% uncertainty. The mean ion concentration of stream water (A, B2, C) lies in the range of expected values for about 80% of surface water in France (Rodier et al., 2009): [F^-] = 0.40 $mg.L^{-1}$ < 1 mg $mg.L^{-1}$; [Cl^-] = 22.2 $mg.L^{-1}$ < 100 $mg.L^{-1}$; [SO_4^{2-}] = 42.2 $mg.L^{-1}$ < 100 $mg.L^{-1}$; [Na^+]= 16.3

310 mg.L^{-1} < 10-500 mg.L^{-1}; [K^+] = 8.3 mg.L^{-1} < 10-15 mg.L^{-1}; [Mg^{2+}] = 6.3 mg.L^{-1} < 15
311 mg.L^{-1}; and [Ca^{2+}] = 22.9 mg.L^{-1} < 25 mg.L^{-1}. Only the mean concentration of nitrate
312 ([NO_3^-] = 19.7 mg.L^{-1} > 15 mg.L^{-1}) could be tied to the agricultural activity present around
313 the La Commanderie area. The phosphate concentrations are below the limit of
314 quantification (< 0.2 mg.L^{-1}).

315 Figure 5 and Table 1 highlight the specific composition of water at Point B1, which has
316 been enriched in F^-, SO_4^{2-}, Mg^{2+} and Ca^{2+} by a mean factor of 3.2, 4.1, 2.8 and 1.9,
317 respectively, in comparison to the average of the other points. This result underscores a
318 difference in the origin of water supplying the trench, which most likely stems from
319 underground or infiltrated waters. This statement confirms the impact of water seepage on
320 Point B1, where the same water composition is observed with concentrations of: [F^-] = 2.6
321 mg.L^{-1}, [SO_4^{2-}] = 179 mg.L^{-1}, [Mg^{2+}] = 7.2 mg.L^{-1}, and [Ca^{2+}] = 16.5 mg.L^{-1}.

322 Acidic water and the high amount of SO_4^{2-} might be due to the acid mine drainage (AMD)
323 process occurring in the waste rock pile (Abdelouas, 2006; Lee *et al.*, 2002). Sulfides,
324 which are common constituents in ore deposits, generate sulfuric acid via oxidation
325 catalyzed by microbial activity. Oxidation can occur in the upper parts of tailings from
326 rainwater infiltration but also in the bottom part due to the connection with underground
327 waters (Abdelouas, 2006; Lee *et al.*, 2002). The origin of sulfide minerals responsible for
328 AMD (usually pyrite) remains unknown at the La Commanderie site because of the
329 prevalence of granitic bedrock. Nevertheless, these minerals may originate from other
330 geological sources, e.g. the materials used for site remediation. The formation of water
331 seepage could be explained by the presence of oxidized zones in the waste rock pile
332 capable of triggering the formation of preferential water pathways through the pile
333 (Boekhout *et al.*, 2015).

334 Seasonal changes in the major components occur mainly during the LF period for Point B1
335 due to water stagnation in the trench. This stagnation during the LF period induces changes
336 in other parameters, namely: a sharp decrease in the dissolved O_2 concentration
337 accompanied by the formation of HCO_3^-, and an increase in both DOC and conductivity
338 (growth of microorganisms). These changes produce reductive conditions in the trench
339 between Points B1 and B2 (50 mV/NHE). At Point A, the input of a large amount of DOC
340 with a maximum value of 51 mg.L^{-1} (December 2016) could be attributed to agricultural

activities (specifically cattle farming), which also leads to a decrease in redox potential (131 mV/NHE).

For F^-, SO_4^{2-}, Mg^{2+} and Ca^{2+} concentrations, an upstream-downstream gradient on the stream was observed during both HF periods (hydraulic connection between the trench and the stream), thus demonstrating the chemical influence of water seepage up to Point A. The spatial and temporal variations observed for water quality parameters (pH, Eh, DOC and $[SO_4^{2-}]$) constitute key factors controlling U speciation and its lability in water.

4.4. Behavior of radionuclides and trace elements in water

Trace element analyses on dissolved fractions are reported in Table 2, with the total fractions listed in SI-5. To simplify the discussion, mean results per flow period are preferred to monthly results, with a distinction made between sampling points and high and low-flow periods. The measured concentrations in Cu and Pb were very low in all water samples with respect to the limit of quantification; therefore, these values will not be discussed. No uranium retention onto filters was observed with 0.45 µm, 0.1 µm and 0.02 µm filters by means of repeated analyses of water samples from Point C filtered twice successively with a new filter on the same cutoff.

Table 2:Mean dissolved concentrations (< 0.45 µm) of trace elements (with SD in brackets) in the La Commanderie stream at sampling Points C, B1, B2 and A during 3monitoring periods, as well as in the water seepage (WS, n=1) in March 2018.

Element (< 0.45 µm)			**[Mn] mg.L^{-1}**			**[Fe] mg.L^{-1}**		
Site/Flow period			HF1	LF	HF2	HF1	LF	HF2
C			0.04 (0.01)	0.1 (0.06)	0.02 (0.02)	0.12 (0.05)	0.14 (0.1)	0.06 (0.05)
B1			0.24 (0.07)	2.7 (1.2)	2.7 (1)	1.01 (0.06)	29 (20)	15 (10)
B2			0.08 (0.01)	0.18 (0.06)	0.13 (0.04)	0.35 (0.03)	0.4 (0.3)	0.4 (0.3)
A			0.09 (0.03)	0.2 (0.11)	0.15 (0.01)	0.22 (0.003)	0.43 (0.3)	0.5 (0.07)
WS			1.0	-	-	0.12	-	-
[Sr] µg.L^{-1}			**[As] µg.L^{-1}**			**[U] µg.L^{-1}**		
HF1	LF	HF2	HF1	LF	HF2	HF1	LF	HF2
49 (11)	90 (46)	66 (10)	5.4 (0.3)	20 (15)	1.9 (1.2)	14 (2)	16 (6)	9 (1)
61 (18)	166 (42)	138 (24)	3.1 (1.3)	16 (3.4)	2.5 (2.3)	139 (30)	80 (26)	34 (7)
55 (11)	87 (32)	81 (6)	3.1 (1.8)	17 (15)	1.3 (1.1)	76 (18)	18 (4)	16 (4)
59 (11)	94 (31)	87 (4)	2.7 (1.3)	22 (10)	1.4 (1.4)	59 (13)	20 (9)	10 (2)
112	-	-	5.8	-	-	436	-	-

361 *4.4.1. Variation of other elements: Sr, Mn, Fe, and As*

362 For Sr and Mn, the average ratio of total to dissolved concentrations is calculated to equal
363 1, thus indicating that these elements are in dissolved form, whereas 41% and 47% of the
364 Fe and As species were measured in particulate form. These two elements are therefore
365 being transported as dissolved and particulate forms into the stream.

366 The Sr concentrations, which range from 49 to 166 $\mu g.L^{-1}$, are of the same order of
367 magnitude for all four sampling points and every sampling period, including the spot
368 sample at the WS location. Sr is a stable element with a simple chemistry and exists mainly
369 as dissolved Sr^{2+} (Rodier et al., 2009). Nevertheless, a slight increase is noticed at Point B1
370 during the LF period, which could be explained by water stagnation and enrichment by
371 evaporation in the trench, with an average concentration factor of 1.8 during the LF period
372 in comparison to the average value at the other points (C, B2, A). These results are
373 consistent with ion concentration analyses (Fig. 5).

374 An increase in dissolved concentrations of the other trace elements was identified at Point
375 B1, in contrast with the other points, by a mean factor of 47 for Fe and 16 for Mn.
376 Concerning As, the specificity (increase by a factor 3.2) of Point B1 was only noticed
377 when considering the total concentration (SI-5) but remained insignificant when
378 considering the dissolved concentrations (Table 2). These values are higher than the
379 concentration factors observed for Sr, which suggests that either these elements were
380 introduced into the trench by water seepage or a change in speciation occurs in the trench.

381 The mean concentration of Fe at Point B1 during the HF1 period equaled 1.01 $mg.L^{-1}$
382 compared to 29 $mg.L^{-1}$ during the LF period (Table 2). These values are higher than the
383 concentration measured in water seepage ([Fe] =0.12 $mg.L^{-1}$) yet are consistent with the
384 presence of a large amount of orange precipitate observed in the trench. This phenomenon
385 is characteristic of AMD, when soluble Fe^{3+} ions in low pH water precipitate as $Fe(OH)_3$ in
386 contact with freshwater in the trench close to neutral pH (Lee *et al.*, 2002). Other types of
387 iron precipitates, such as iron oxides, oxyhydroxides and iron-oxyhydroxysulfates, can also
388 be observed in such cases (Lee *et al.*, 2002; Salbu *et al.*, 2013). During the LF period, a
389 reverse phenomenon was observed with reducing conditions in the trench, i.e. conversion
390 of $Fe(OH)_3$ precipitate into Fe^{2+} dissolved species, hence considerably increasing the local
391 concentration of Fe at Point B1. As opposed to Fe, Mn is present only as dissolved species,

392 a finding that is consistent with the study by Lee et al., who demonstrated that Mn oxides
393 do not form from different AMD waters for pH values below 7.

394 The measured dissolved concentration of As in the water seepage is quite low, i.e. 5.8
395 $\mu g.L^{-1}$, and lies very close to the mean concentrations measured at Point B1 during both
396 HF1 (3.1 $\mu g.L^{-1}$) and HF2 (2.5 $\mu g.L^{-1}$). During the LF period, higher concentrations of As
397 were detected for all sampling points, ranging from 16 to 22 $\mu g.L^{-1}$, with a significantly
398 higher concentration at B1 in considering the total concentration (59 $\mu g.L^{-1}$ vs. a mean
399 concentration of 22 $\mu g.L^{-1}$ for C, B2 and A). Since no hydraulic connection had been
400 established with the trench during the LF period, a direct contamination from the water
401 seepage could be excluded; however, a change in As speciation occurs in the trench. The
402 mobility of As is quite complex and greatly influenced by redox conditions, the sorption
403 process on Fe oxides and microorganisms (Casiot *et al.*, 2009; Dinsdale *et al.*, 1992).
404 Briefly, the increase in temperature during summer favors the development of anoxic or
405 suboxic conditions in sediments and moreover boosts bacterial activity. These conditions
406 favor the reduction of oxide phases and the mobilization of associated metals, metalloids
407 and especially As in the Garonne-Dordogne Basin (Masson *et al.*, 2007). This process
408 seems likely for the La Commanderie site, but further investigation into the speciation of
409 As is needed to confirm this hypothesis.

410 *4.4.2. Source, behavior and regulations regarding Uranium in the stream*

411 Uranium was monitored as the primary marker of the impact on the La Commanderie site
412 as regards the mine's operating history. The geochemical background of U was estimated
413 by Salpeteur and Angel from surface water samples covering 120 rivers in France, and a
414 value of 0.15$\mu g.L^{-1}$ of dissolved U was selected for the Hercynian area. However,
415 concentrations from reference point C and water monitored upstream (RNM,
416 Environmental Radioactivity Measurements in France) lie in the range of 5-30 $\mu g.L^{-1}$, thus
417 indicating a higher local geochemical background.

418 The dissolved concentration of U was measured on average at 3.4 times higher for Point
419 B1, in comparison to the other points (C, B2, A). During HF1, the mean U concentration at
420 Point B1 was 139 $\mu g.L^{-1}$, in contrast with a water seepage concentration measured at 436
421 $\mu g.L^{-1}$. The direct input from water seepage is obvious relative to the flow rate and lower
422 concentration for other points (Table 2). Acid mining drainage is suspected to occur in the

423 uranium ore deposit, hence releasing toxic metals into the immediate environment. Both U
424 and Fe are mobilized from the oxidized parts of the tailings pile into the water seepage.
425 Then, Fe precipitation in the trench with a change of pH acts as an efficient scavenger for
426 Mn, As and U (Abdelouas, 2006; Casiot *et al.*, 2009; Duff *et al.*, 2002). Investigations into
427 the U content of sediments in the trench could be beneficial as regards the results from
428 Salbu *et al*., who recorded high concentrations of ^{238}U in such Fe precipitates (around 1.85
429 g/kg) at the Kurday uranium mining site in Kazakhstan.

430 This result is consistent with the local anomaly detected using gamma-ray mapping (Fig. 4)
431 to identify water seepage as the direct contributor to the radionuclide leak in the
432 environment and mainly natural U with gamma emitters in the ^{238}U decay chain (^{234}Th,
433 ^{234m}Pa, ^{226}Ra, ^{214}Pb, ^{214}Bi, ^{210}Pb). However, the origin of water seepage flowing into the
434 trench at Point B1 remains unknown and could be due either to the water from the basin
435 relative to the basin water level during high-flow periods or to the rainfalls that slowly
436 infiltrate the tailing pile (Abdelouas, 2006).

437 As for the other elements from water seepage, a global downward trend of U concentration
438 was noticed for water flow periods HF1 and HF2 from Points C to A. Downstream of Point
439 A, the U concentration decreases due to dilution in the "Boisdroitière" stream. The impact
440 of the former mining activity on water becomes less visible, although particular events
441 such as heavy rains could mobilize U in particulate form.

442 The French regulation regarding nuclear management, as revised in June 2018 (French
443 decree 2018-434), does not assign a limit for U concentration in industrial or mining water
444 discharge into the environment but does impose a continuous monitoring of uranium
445 concentrations. In practice, a maximum value of 1,800 µg L^{-1} (23.4 Bq.L^{-1}) appears for
446 discharge authorizations adopted by local authorities based on Orano (formerly AREVA)
447 expertise. The highest U concentration measured in water seepage ([U] = 436 µg L^{-1}),
448 characterizing the interface between the waste rock pile and the environment, lies below
449 this value. For the sake of comparison, a tighter control is applied in the U.S. and Brazil,
450 with legal limits set respectively at 85 µg.L^{-1} (1.1 Bq.L^{-1}) and 31 µg.L^{-1} (0.4 Bq.L^{-1})
451 (Carvalho *et al.*, 2005). The environmental reference, as represented by the Annual
452 Average Quality Standard for freshwater organisms (AA-$QS_{fw,eco}$), was set at a value of 0.3
453 µg.L^{-1} for uranium (EU Water Framework Directive) in non-contaminated areas. In areas
454 with a significant geochemical background (e.g. granitic areas), this value is added to the

455 geochemical background value to calculate the AA-$QS_{fw,eco}$. For the La Commanderie
456 case, this value is of the same order of magnitude as the regional geochemical background
457 (0.15 µg.L^{-1}) yet also 6,000 times less than the local authorized value, which challenges the
458 pertinence of environmental protection reference values. In addition, the Technical
459 Guidelines for Deriving Environmental Quality Standards, TGD-EQS (EU 2011),
460 recommends taking into account both metal bioavailability and speciation. In this study
461 therefore, the labile part of U in water was investigated by fractionation and DGT
462 techniques.

463 *4.4.3. Fractionation of Uranium by filtration and the DGT labile part*

464 The results of the fractionation of aqueous uranium species using filtration and DGT
465 techniques are displayed in Figure 6. The uncertainty, expressed as a confidence interval (α
466 = 0.05), of U concentrations was calculated at 15% for spot water sampling and at 35% for
467 DGT sampling, in accounting for replicates and the propagation of analytical error
468 variance following Gaussian error propagation laws.

469 The distribution of U among the total and dissolved fraction (0.45 µm) (Table 2 and SI-5)
470 at the various stream locations (C, B2, A) does not vary substantially with respect to
471 uncertainty and variability, with a concentration ratio of 0.92, which means that U is
472 mainly being transported in dissolved or colloidal form. Nevertheless, during HF periods, a
473 decreasing trend in U concentrations with the lowest filtration cutoff (especially the range
474 between 0.1 and 0.02 µm) suggests a partition between dissolved and small colloidal
475 forms, most likely with humic aggregates from NOM present at each sampling point (Lead
476 and Wilkinson, 2006).

477 Uranium DGT-labile concentrations were in accordance with a dissolved U fraction (<
478 0.45 µm). This result is consistent with the ability of DGT to integrate a large panel of
479 metal complexes naturally occurring in freshwater as free metals, inorganic complexes and
480 small organic complexes (Zhang and Davison, 2015). Moreover, U in colloidal form,
481 between 0.1 µm and 0.02 µm, was also integrated by DGT. Therefore, in the La
482 Commanderie stream, dissolved U (< 0.45 µm) can be considered as labile and potentially
483 bioavailable U species for the aquatic ecosystem. DGT derived concentrations can be
484 directly compared with AA-$QS_{fw,eco}$ values.

485

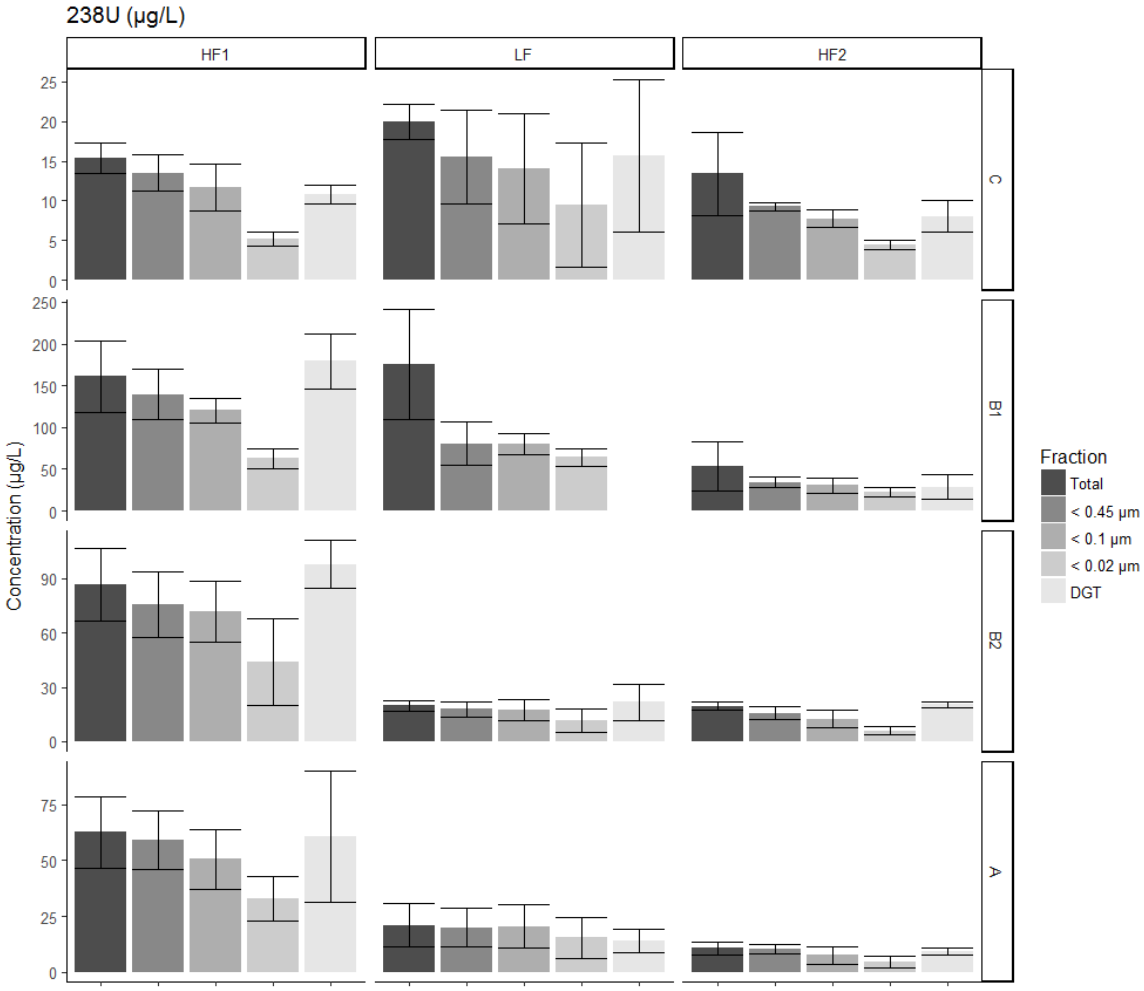

Figure 6: Concentrations of uranium in raw, 0.45 µm, 0.1 µm and 0.02 µm filtered water samples and DGT-labile concentrations over the three monitoring periods (period variability expressed as a standard deviation)

At Point B1 however, the proportion of U in particulate form (with a size greater than 0.45 µm) was fluctuating between 14%, 54% and 36% for the HF1, LF and HF2 periods, respectively. In the LF period, this difference is correlated with the presence of orange particles arising from the precipitation of Fe in the trench and a higher DOC content. U is probably being sorbed onto large particles of Fe oxy-hydroxides and complexes with NOM (Duff *et al.*, 2002). It is also possible that U(VI) soluble species are reduced and then co-precipitated as less soluble U(IV) species by metal-reducing bacteria during the LF period (Duff *et al.*, 2002).

The overall agreement between DGT and water concentrations is satisfactory. This conclusion has also been validated for Point B1, which is the most heavily influenced by

501 former mining operations, even though no DGT samplers were deployed at B1 during the
502 LF period due to unsuitable field conditions (stagnant water in the trench). The use of DGT
503 under environmental conditions, and specifically AMD waters, seems to be relevant, as has
504 been reported in other studies (Casiot *et al.*, 2009). As a drawback of the DGT technique,
505 measurement variability is greater than with the water spot sampling technique due to
506 higher global calculation uncertainties.

507 5. Conclusion

508 A radiological investigation in the area surrounding the former La Commanderie uranium
509 mine has been carried out in order to identify the environmental footprint. The proposed
510 methodology, which combines gamma-ray mapping, water sampling and chemical analysis
511 (including DGT measurements), has provided fresh insight into describing U transport in
512 the environment. Gamma-ray mapping allows identifying water seepage from the waste
513 rock pile as a potential leak of radionuclides into the environment. Monitored water
514 seepage showed low pH (4.2), high sulfate content (179 $mg.L^{-1}$) and high U concentrations
515 of up to 436 $\mu g.L^{-1}$, which indicate that an acid mining drainage (AMD) process is
516 occurring either inside or under the oxidized parts of the waste rock pile. Monitoring data
517 over three flow periods revealed a higher U release during the high-flow period in the La
518 Commanderie stream up to Point A, which is compliant with local regulations. Based on
519 DGT measurements, the dissolved part of the U released is considered as labile, with
520 concentrations exceeding environmental standards for freshwater organisms. AMD is also
521 responsible for releases in the immediate environment of a non-negligible amount of Fe,
522 Mn and As in both dissolved and particulate form.

523 In future studies, specific scientific concerns for the La Commanderie site should focus
524 both on the connection between the basin and the water seepage and on sediments in the
525 trench as interfaces between the mining site and the environment. Subsequent efforts
526 should be devoted to: i) determining the actual origin of the water seepage, ii)
527 understanding the transport mechanisms occurring in the waste rock pile, and iii) tracking
528 the evolution of uranium release from the water seepage over time. Nevertheless, as a
529 potential connection with the basin is strongly suspected here, such a hypothesis, if
530 confirmed, would have to be taken into account in a future water management plan. It is

noteworthy that in June 2018, works to channel the water seepage properly into the stream were performed in order to avoid overflowing on the footpath (SI-2).

The present work highlights the influence of flow periods on the release of uranium from AMD waters as an important factor for modeling their environmental impact and developing strategies for former uranium mines management. Furthermore, changes in dissolved oxygen concentration and redox potential during low flow periods modify the speciation of Fe (in AMD waters) which acts as a scavenger for other elements such as As, Mn and U. The use of DGT under environmental conditions, and specifically AMD waters, seems to be relevant in comparison to filtered spot water sampling strategies for assessing the labile fraction of U in impacted waters.

6. Acknowledgments

[redacted]

7. References

Abdelouas, A., 2006. Uranium mill tailings: Geochemistry, mineralogy, and environmental impact. Elements 2, 335-341.

AREVA, 2013. Bilan environnemental - Sites miniers de Vendée. AREVA Mines, p. 145.

Boekhout, F., Gerard, M., Kanzari, A., Michel, A., Dejeant, A., Galoisy, L., Calas, G., Descostes, M., 2015. Uranium migration and retention during weathering of a granitic waste rock pile. Applied Geochemistry 58, 123-135.

Carvalho, I.G., Cidu, R., Fanfani, L., Pitsch, H., Beaucaire, C., Zuddas, P., 2005. Environmental impact of uranium mining and ore processing in the Lagoa Real District, Bahia, Brazil. Environmental Science & Technology 39, 8646-8652.

Casiot, C., Egal, M., Elbaz-Poulichet, F., Bruneel, O., Bancon-Montigny, C., Cordier, M.A., Gomez, E., Aliaume, C., 2009. Hydrological and geochemical control of metals and arsenic in a Mediterranean river contaminated by acid mine drainage (the Amous River, France); preliminary assessment of impacts on fish (Leuciscus cephalus). Applied Geochemistry 24, 787-799.

Chapot, G., Croupie, R., Dumas, J., Leblanc, P., Kerouanton, J.-L., 2010. L'Uranium Vendéen.

Cuvier, A., Panza, F., Pourcelot, L., Foissard, B., Cagnat, X., Prunier, J., Van Beek, P., Souhaut, M., Le Roux, G., 2015. Uranium decay daughters from isolated mines: Accumulation and sources. Journal of Environmental Radioactivity 149, 110-120.

Dinsdale, B.E., Belin, D.D., Altringer, P.B., 1992. Biological arsenic removal from mining and milling waters by anaerobic sulfate-reducing bacteria. Environmental Issues and Management of Waste in Energy and Mineral Production, Vols 1 and 2, 1389-1400.

Drozdzak, J., Leermakers, M., Gao, Y., Elskens, M., Phrommavanh, V., Descostes, M., 2016a. Uranium aqueous speciation in the vicinity of the former uranium mining sites using the diffusive gradients in thin films and ultrafiltration techniques. Analytica Chimica Acta 913, 94-103.

Drozdzak, J., Leermakers, M., Gao, Y., Phrommavanh, V., Descostes, M., 2015. Evaluation and application of Diffusive Gradients in Thin Films (DGT) technique using Chelex (R)-100, Metsorb (TM) and Diphonix (R) binding phases in uranium mining environments. Analytica Chimica Acta 889, 71-81.

Drozdzak, J., Leermakers, M., Gao, Y., Phrommavanh, V., Descostes, M., 2016b. Novel speciation method based on Diffusive Gradients in Thin Films for in situ measurement of uranium in the vicinity of the former uranium mining sites. Environmental Pollution 214, 114-123.

Duff, M.C., Coughlin, J.U., Hunter, D.B., 2002. Uranium co-precipitation with iron oxide minerals. Geochimica Et Cosmochimica Acta 66, 3533-3547.

Franke, K., Rossler, D., Gottschalch, U., Kupsch, H., 2000. Mobilization and retardation of uranium DOC species at three mine piles in Schlema/Alberoda, Saxony, Germany. Isotopes in Environmental and Health Studies 36, 223-239.

596 Gimpel, J., Zhang, H., Hutchinson, W., Davison, W., 2001. Effect of solution composition,
597 flow and deployment time on the measurement of trace metals by the diffusive gradient in
598 thin films technique. Analytica Chimica Acta 448, 93-103.

599 Gregusova, M., Docekal, B., 2011. New resin gel for uranium determination by diffusive
600 gradient in thin films technique. Analytica Chimica Acta 684, 142-146.

601 Hutchins, C.M., Panther, J.G., Teasdale, P.R., Wang, F.Y., Stewart, R.R., Bennett, W.W.,
602 Zhao, H.J., 2012. Evaluation of a titanium dioxide-based DGT technique for measuring
603 inorganic uranium species in fresh and marine waters. Talanta 97, 550-556.

604 Landa, E.R., Gray, J.R., 1995. US geological survey-research on the environmental fate of
605 uranium mining and milling wastes. Environmental Geology 26, 19-31.

606 Lead, J.R., Wilkinson, K.J., 2006. Aquatic colloids and nanoparticles: Current knowledge
607 and future trends. Environmental Chemistry 3, 159-171.

608 Lee, G., Bigham, J.M., Faure, G., 2002. Removal of trace metals by coprecipitation with
609 Fe, Al and Mn from natural waters contaminated with acid mine drainage in the Ducktown
610 Mining District, Tennessee. Applied Geochemistry 17, 569-581.

611 Masson, M., Schafer, J., Blanc, G., Pierre, A., 2007. Seasonal variations and annual fluxes
612 of arsenic in the Garonne, Dordogne and Isle Rivers, France. Science of the Total
613 Environment 373, 196-207.

614 Menegario, A.A., Yabuki, L.N.M., Luko, K.S., Williams, P.N., Blackburn, D.M., 2017.
615 Use of diffusive gradient in thin films for in situ measurements: A review on the progress
616 in chemical fractionation, speciation and bioavailability of metals in waters. Analytica
617 Chimica Acta 983, 54-66.

618 Pereira, W.D., Kelecom, A., da Silva, A.X., do Carmod, A.S., Py, D.D., 2018. Assessment
619 of uranium release to the environment from a disabled uranium mine in Brazil. Journal of
620 Environmental Radioactivity 188, 18-22.

621 Rodier, J., Legube, B., Merlet, N., Brunet, R., 2009. L'analyse de l'eau - 9e éd. - Eaux
622 naturelles, eaux résiduaires, eau de mer. Dunod.

623 Salbu, B., Burkitbaev, M., Stromman, G., Shishkov, I., Kayukov, P., Uralbekov, B.,
624 Rosseland, B.O., 2013. Environmental impact assessment of radionuclides and trace
625 elements at the Kurday U mining site, Kazakhstan. Journal of Environmental Radioactivity
626 123, 14-27.

627 Salpeteur, I., Angel, J.M., 2010. Geochemical baseline data for trace elements in surface
628 water and active sediment from French rivers collected by the FOREGS Geochemical
629 Atlas of Europe (I). Environnement Risques & Sante 9, 121-135.

630 Turner, G.S.C., Mills, G.A., Teasdale, P.R., Burnett, J.L., Amos, S., Fones, G.R., 2012.
631 Evaluation of DGT techniques for measuring inorganic uranium species in natural waters:
632 Interferences, deployment time and speciation. Analytica Chimica Acta 739, 37-46.

633 Zhang, H., Davison, W., 2015. Use of diffusive gradients in thin-films for studies of
634 chemical speciation and bioavailability. Environmental Chemistry 12, 85-101.

635